



Smartphone controlled interactive portable device for theranostics in vitro

Sunil Kumar Sailapu^{a,1}, Deepanjalee Dutta^{a,2}, Anitha T. Simon^a, Siddhartha Sankar Ghosh^{a,b,**}, Arun Chattopadhyay^{a,c,*}

^a Centre for Nanotechnology, Indian Institute of Technology Guwahati, Guwahati 781 039, Assam, India

^b Department of Biosciences and Bioengineering, Indian Institute of Technology Guwahati, Guwahati 781 039, Assam, India

^c Department of Chemistry, Indian Institute of Technology Guwahati, Guwahati 781 039, Assam, India



ARTICLE INFO

Keywords:

Colorimetric assays
Diagnosis
LED
Portable device
Photodynamic therapy
Smartphone
Theranostics

ABSTRACT

In this work, a smartphone controlled interactive theranostic device has been developed to perform in vitro photodynamic therapy (PDT) and diagnostic assays for treatment assessment on a single platform. Further, silver nanorod (Ag NR) was identified as a photosensitizer and its effect was studied in three different cell lines. PDT was achieved with Ag NRs using low irradiation (1.4 mW/cm² at 632 nm) from light emitting diodes (LEDs) in the device. Specifically, PDT in conjugation with widely used chemotherapeutic drug doxorubicin (Dox) proved effective in killing of HeLa cancer cells and multicellular tumor spheroids at a minimum dose of Ag (2.5 µg/mL). The MTT (3-(4,5-dimethylthiazol-2-yl)-2,5-diphenyltetrazolium bromide) and LDH (lactate dehydrogenase) assays performed with the device indicated the therapeutic success of the delivered PDT. The device is portable and can be adapted for different wavelength irradiations and radiation doses. Additionally, wireless operation using a custom designed smartphone application makes it convenient to use in complex environments without much of human intervention.

1. Introduction

The burden of disease such as cancer gets magnified in remote locations, owing primarily to high cost of detection and complex procedures. In this regard, high throughput, low cost point-of-care (POC) platforms can be particularly advantageous when ambulatory treatment is desired (Dhawan, 2016). Besides, accelerated failure rate of conventional chemotherapy suggests need for alternative approaches (Komarova and Boland, 2013; Nahabedian et al., 1988).

Amongst the popular techniques, PDT is a clinically approved form of treatment-based on activation of suitable photosensitizers, at the site of treatment, using light of wavelengths in the biological window (600–900 nm) (Muller and Wilson, 1986). PDT is minimally invasive and has several advantages such as early recovery and no requirement of systematic treatment, in comparison to surgery and radiotherapy (Rodrigues et al., 2019). Unlike photothermal therapy (PTT), it is also

not affected by other parameters such as temperature fluctuations that could result in undesired outcomes. Commercial organic photosensitizers used in PDT, however suffer from drawbacks related to photo-degradation, stability and toxicity, single wavelength excitation and enzymatic degradation (Huang et al., 2011; Yogo et al., 2005). Importantly, their low extinction coefficients demand high dosage of organic photosensitizers and powerful light sources, which limit their POC applications. Alternatively, optically tuneable nanomaterials with photosensitizing ability, i.e., to generate singlet O₂ upon irradiation with light corresponding to the localized surface plasmon resonance (LSPR) bands (Vankayala et al., 2014), offer distinguishable advantages such as resistance to enzymatic and photo degradations over organic photosensitizers. In addition, the high extinction coefficient of the nanomaterial would allow PDT at reduced doses and low irradiations with feasibility for tuneable wavelength excitation. On the other hand, combination therapy involving PDT can provide synergistic effects

* Corresponding author. Department of Chemistry, Indian Institute of Technology Guwahati, Guwahati 781 039, Assam, India.

** Corresponding author. Department of Biosciences and Bioengineering, Indian Institute of Technology Guwahati, Guwahati 781 039, Assam, India.

E-mail addresses: sunil.sailapu@imb-cnm.csic.es (S.K. Sailapu), deepanjalee.dutta@ed.ac.uk (D. Dutta), sailapu@iitg.ac.in (S.S. Ghosh), arun@iitg.ac.in (A. Chattopadhyay).

¹ S. K. S. is now with Instituto de Microelectrónica de Barcelona, IMB-CNM (CSIC), C/del Til·lers., Campus Universitat Autònoma de Barcelona (UAB), 08193 Bellaterra, Barcelona, Spain.

² D. D. is now with School of Chemistry, Joseph Black Building, University of Edinburgh.

especially in combatting multidrug resistance (Nahabedian et al., 1988; Zhang et al., 2017). The relatively employed chemotherapeutic drug dosage during combinatorial treatment could be effectively reduced if the involved photosensitizer could induce pronounced PDT. In this regard, shape dependent LSPR in Ag nanorods (NRs) may be efficient in the formation of singlet O_2 species upon absorbing light of wavelengths in the biological window. Though, many nanoparticles have been used for PDT, the application or potential of Ag NRs as photosensitizer has not been exploited.

Low power/irradiance and thermally non-destructive LEDs can be alternatives to high power lasers/LEDs (Guo et al., 2015; Hartl et al., 2015) to develop simpler POC devices with minimum components. Additionally, they could still achieve singlet O_2 generation if used in conjunction with high extinction coefficient based materials. Further, these wavelength tuneable LED sources offer viable options with regard to conjugation of colorimetric diagnostic assays in an easy approach (Luka et al., 2017). This integration is valuable as often after a cancer therapeutic regime is put into effect, the state of treated cells has to be analysed using (primarily) colorimetric based biochemical assays that include ELISA, MTT, LDH, and alamarBlue (AB) (Merlin et al., 1992). In recent days, microplate readers linked with smartphones are being developed as portable and cost-effective devices for diagnostic assays (Berg et al., 2015; Kwon et al., 2016). However, it would be far more effective if portable POC devices are equipped with multifunctional capabilities so as to achieve a theranostic function by performing both therapy and subsequent treatment evaluative diagnostic routines.

Herein, we present a smartphone based portable device capable of achieving a theranostic function by carrying out in vitro PDT at low irradiation doses using LEDs and also to subsequently perform colorimetric biochemical assays for assessing the therapeutic success in a 96-well plate format (Fig. 1a). We also identified that Ag NRs can act as photosensitizers by themselves and mediate killing of HeLa cancer cells at low irradiances (1.4 mW/cm^2) achieved using the device. When these Ag NRs were used with chemotherapeutic drug Dox, achievement of combinatorial therapy at low dosages of Ag ($2.5 \text{ }\mu\text{g/mL}$) and irradiances was possible. Using the POC device, quantification of cell viability was also achieved based on MTT and LDH assays following the treatment. In addition, the efficacy of the combined photochemotherapy was pursued in multicellular tumor spheroids in order to evaluate the therapeutic

activity in a solid tumor like environment. The device is promising in terms of delivering ambulatory treatment, screen novel photosensitizers, or to independently perform colorimetric assays and also for being affordable for a larger populace.

2. Material and methods

The details related to materials, characterization studies, cell culture experiments, device assembly, electronic circuit and software app are mentioned in the Supplementary Information.

3. Results and discussion

3.1. Smartphone controlled interactive theranostic device

The smartphone controlled interactive theranostic device consists of a portable case with attachments to package together the optical components and the electronic circuit (Fig. 1b and c). Involving three detachable modules, the device brings together the conjugation of an illumination/irradiation unit and an optical measurement unit within a compact design of overall height approximately 4.5 cm. PDT is delivered through the switchable LED array (Fig. 1d, Video S1) in the illumination unit to the samples contained in the 96-well plate placed above it. However, during optical measurements for diagnostic assays such as MTT and LDH, the illumination unit acts as an incident light for the analysed samples in each well of the plate. The phototransistor array in the measurement unit provides the absorbance values of 96 samples in a single scan by measuring the transmitted light through the samples. The device is wirelessly operated through a smartphone based app (Fig. 1e) that features input parameters and also provides digital output readings of measured values.

Supplementary data related to this article can be found at <https://doi.org/10.1016/j.bios.2019.111745>.

The thermal and optical characteristics of the device was evaluated prior to its implementation for PDT related applications. In case of LEDs (632 nm LED for PDT, 570 nm LED for MTT, 470 nm LED for LDH) used in the present work, good stability of irradiation power was observed when operated for a period of 30 min (Fig. S1). Further, the temperature of the LEDs was also found to be relatively stable as significant changes

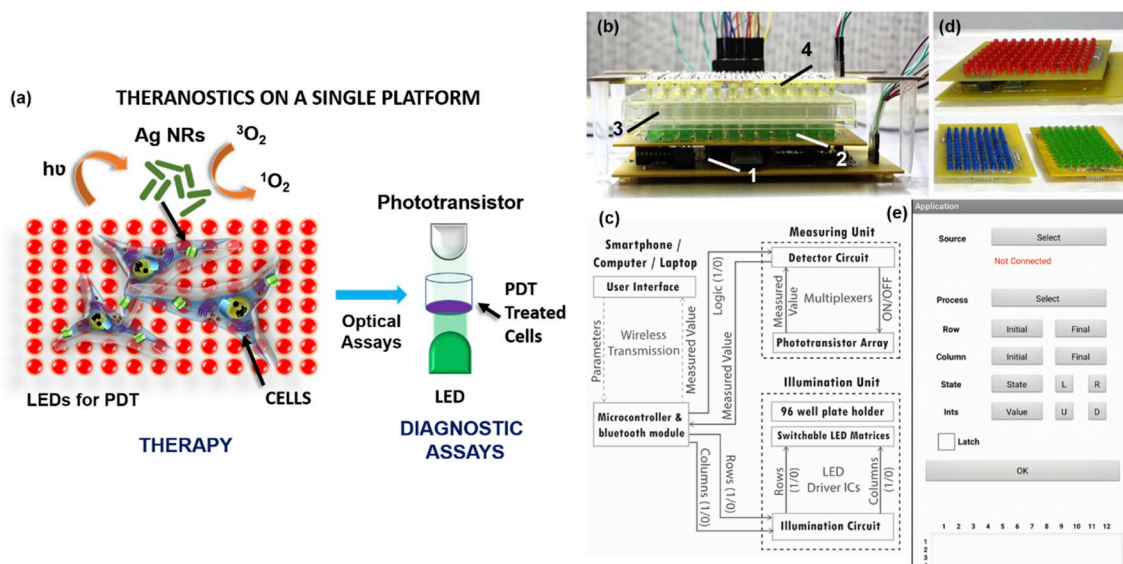


Fig. 1. Smartphone controlled interactive theranostic device. (a) The scheme illustrates the application of low power LEDs for PDT, and also to perform diagnostic assays on a single platform. PDT was demonstrated in cancer cells using Ag NRs as photosensitizer to generate singlet O_2 upon irradiation with LEDs. The therapeutic efficiency was monitored by optical assays such as MTT, LDH using combination of LEDs and phototransistors. (b) Image of the device used for pursuing PDT and to perform optical based assays. Here, (1, 2, 3, 4) represent electronic circuit, LED array, 96-well plate and phototransistor array. (c) Flow chart describing various units and interconnections. (d) Switchable LED arrays. (e) Smartphone app to operate the device and to acquire output data.

from room temperature have not been observed. The photocurrent of the phototransistor was found to change linearly with the illuminance of light falling on it, thus enabling the measurement of the transmitted light. Overall, the performance characteristics of the device suggested its favorable application for PDT as well as colorimetric assays.

3.2. Ag NR as photosensitizer for PDT

The *in vitro* PDT performance of the device was evaluated by studying the effect of the low irradiation from LEDs towards promotion of singlet O₂ generation by investigating Ag NRs as potent photosensitizer. The UV-Vis characterization of the as synthesized Ag NRs indicated strong absorbance at 420 nm and 632 nm (Fig. S2a) due to transverse and longitudinal plasmon resonances of the NRs. However, for PDT, we chose wavelength corresponding to 632 nm, so as to achieve better penetration capability with biological samples. Thereby, in order to photo-irradiate Ag NRs to sensitize the formation of singlet O₂, LEDs with peak emission at this LSPR absorption band (Fig. S2b) was used. Further, the formation of the Ag NRs with an average aspect ratio of 3.71 ± 0.58 nm (calculated by considering multiple images) was confirmed by transmission electron microscopy (TEM) analysis (Fig. S2c) and the presence of Ag was ascertained in the sample with energy dispersive X-ray spectroscopy (EDX) (Fig. S3).

To examine the effect of Ag NRs as photosensitizer, the formation of singlet O₂ in their presence was monitored by 1, 3 - diphenylisobenzofuran (DPBF), which is known to be specific towards singlet O₂ detection. A gradual decrease (~53%) in emission relating to DPBF (Fig. S4) was observed in case of Ag NRs under irradiation (632 nm light), possibly due to the generation of singlet O₂ and breakdown of DPBF. This observation is similar to the quenching phenomena observed in presence of single O₂ reported previously (Huang et al., 2013). Further, when the assay was performed under N₂ purging, this decrease was reduced to ~23%. However, a decrease of luminescence emission up to 72% was observed when purged with O₂. Similar experiments with only DPBF (in absence of Ag NRs) under irradiation, or DPBF in presence of Ag NRs without irradiation did not result in noticeable decay in luminescence. The DPBF assay results revealed that Ag NRs were able to

favorably sensitize the formation of singlet O₂ when irradiated at longitudinal band of LSPR wavelength. Also, the contribution of photo-thermal effect due to the irradiation of the Ag NRs was evaluated by examining the time dependent change in the temperature of the solution. The results showed no significant photothermal activity of the Ag NRs as drastic changes in temperature were not observed (Fig. S5) unlike other nanorods systems based on different nanomaterial composition and excitation conditions (Popp et al., 2014).

3.3. Device application for *in vitro* PDT using Ag NRs, and subsequent diagnostic assays

Having identified the singlet O₂ generation capabilities of Ag NRs, we then explored the possibility of their use for PDT of cancer cells *in vitro*. To perform this with the current device, LED array of 632 nm wavelength was used. Also, the further assessment of the treatment through biochemical assays such as MTT and LDH was carried out with the device (using LED array of wavelength 470, 570 nm). The initial MTT based cell viability studies with Ag NRs in HeLa cells (without irradiation) indicated that around 90% of the cells were viable at 2.5 µg/mL of Ag (Fig. 2a and b). This suggested that Ag NRs had negligible cytotoxic effect on HeLa cells under no irradiation, at this concentration. However, the viability decreased to 63% in case of irradiated samples at the same dosage of Ag. This further decrease may be attributed to the contribution from cell death mediated through generated singlet O₂ by Ag NRs under irradiation, resulting in PDT. We observed that PDT (with Ag NRs), when combined with Dox, enhanced the efficiency of the treatment. For example, the viability of cells after being irradiated in the presence of Ag NRs and then treated with Dox (8.3 µg/mL) showed a marked decrease to about 41% at only 2.5 µg/mL of Ag. Whereas, at same concentrations, studies with only free Dox, and as well as in presence of Dox with Ag NRs (without irradiation) (Fig. S6a) revealed a greater cell viability of 75% and 68%, respectively.

Also, it was observed that if Ag NRs alone were used (with no irradiation), a relatively higher concentration (4.2 µg/mL of Ag) was required to reduce the viability of cells to 50% (IC₅₀) (Fig. S6b) Hence, combinatorial treatment involving PDT achieved IC₅₀ at a reduced

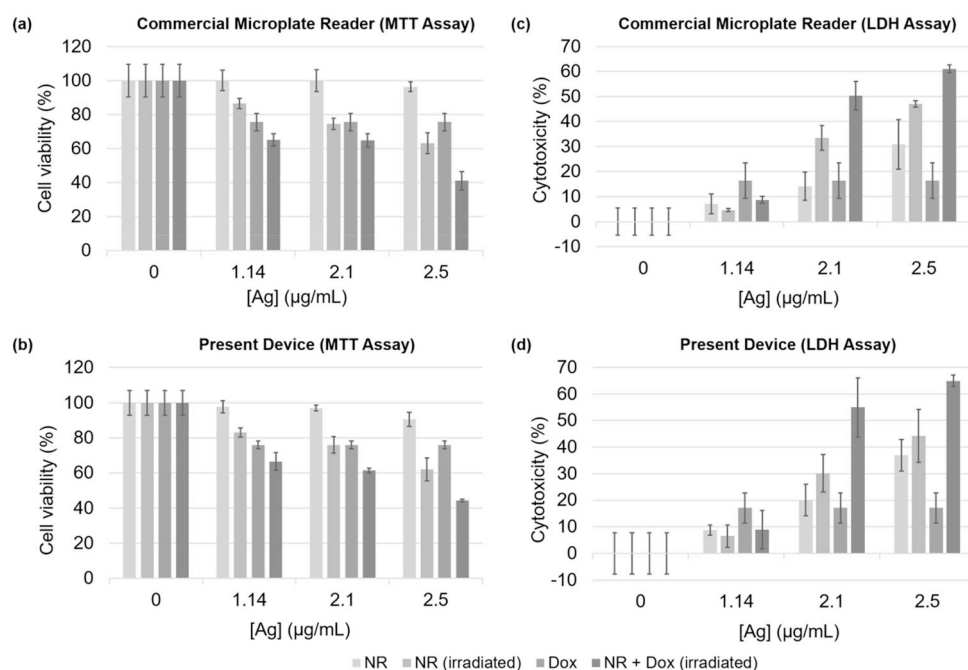


Fig. 2. Comparison of device performance through optical diagnostic assays for cell viability and cell death studies of HeLa cells. Results of MTT and LDH assays performed using (a, c) commercial microplate reader and (b, d) the present device after being subjected to particular treatment as mentioned in the legends. Data is represented as mean and standard deviation from three independent experiments.

dosage of Ag NRs (2.5 µg/mL of Ag) with 8.3 µg/mL of Dox. While relatively high concentrations were reported to achieve efficient killing (IC₅₀) of HeLa cells in Ag nanomaterial based systems (Dutta et al., 2016; Jadhav et al., 2018), the application of PDT in present system helped to reduce the Ag dosage. An irradiation time of 30 min was found to be effective in the combinatorial treatment module to induce optimum cell death. The biocompatibility of the Ag NRs was also assessed in HEK 293T (normal) cells. Around 80% of the cells were observed to be viable at 2.5 µg/mL (dosage used in combinatorial treatment), which indicated the lower toxicity of the Ag NRs towards normal cells (Fig. S6c). Overall, the above results from MTT assay indicated that cell viability could be lowered through combinatorial therapy and signified successful augmentation of conventional chemotherapy with Dox in combination with Ag NR induced PDT. Further, to assess the applicability of smartphone based device in carrying out MTT assay, the values obtained using the device were compared with those measured by conventional microplate reader. The results showed good agreement with the commercial reader and indicated the potential of the device in performing diagnostically relevant optical assays as shown in Fig. 2a and b. The variations in cell viability could be discerned in both devices with the lowest cell viability observed in case of PDT based combinatorial treatment.

In addition, the cell death analysis using LDH assay was performed to complement the cell viability studies. The LDH release from HeLa cells, treated in combination with Ag NRs (upon irradiation) and Dox, was significantly higher in comparison to those treated with Ag NRs (dark) and Dox only (Fig. 2c and d). This suggests more effective cytotoxic effect induced through the application of combination therapy. It was found that the observed trends in cell death obtained from microplate reader and present device showed good agreement where both indicated maximum cell death in combinatorial therapy involving PDT.

The efficacy of the therapy was also analysed in HepG2 and HEK cell lines using MTT and LDH assays (Figs. S7 and S8). Though similar effect was observed in HepG2, the combinatorial activity was less prominent compared to HeLa. Also, in the case of the HEK cells, the therapeutic effect was the least, which is possibly due to the lower uptake capacity of normal cell lines when compared to the greater uptake in cancer cells (due to their higher metabolic activity).

3.4. Determination of intracellular reactive oxygen species (ROS) level to understand cell death mechanism

In order to understand the mechanism involved in cell death, intracellular ROS levels were monitored by dichloro-dihydro-fluorescein diacetate (DCFH-DA) assay in HeLa cells treated with Ag NRs upon irradiation with 632 nm light and also in the dark. An elevation of about ~1.6 times in ROS level was observed in case of irradiated samples by probing DCF fluorescence. Further, to elucidate if the resultant cell death occurred due to the generation of singlet O₂, the intracellular ROS levels were evaluated in HeLa cells, with and without pretreatment of sodium azide (a specific singlet O₂ quencher) before Ag NR treatment. In case of irradiated cells, the results indicated that the ROS level was lowered (by ~17 times) with sodium azide pretreatment. However, for Ag NR treated cells without irradiation, a reduction of only ~1.9 times was observed with sodium azide pre-treatment, as shown in Fig. 3a. The observed greater quenching of ROS levels of sodium azide pretreated samples in presence of irradiation indicated that the cell death was possibly initiated due to Ag NR mediated singlet O₂ generation. Additionally, fluorescence microscopic images also indicated a decrease in fluorescence of DCF due to lowering of the intracellular ROS levels in case of sodium azide pre-treated samples. However, such a decrease in fluorescence was not observed in samples not pre-treated with sodium azide (Fig. 3b–d). This further supported the observations made from the fluorescence-activated cell sorting (FACS) based analysis in Fig. 3a.

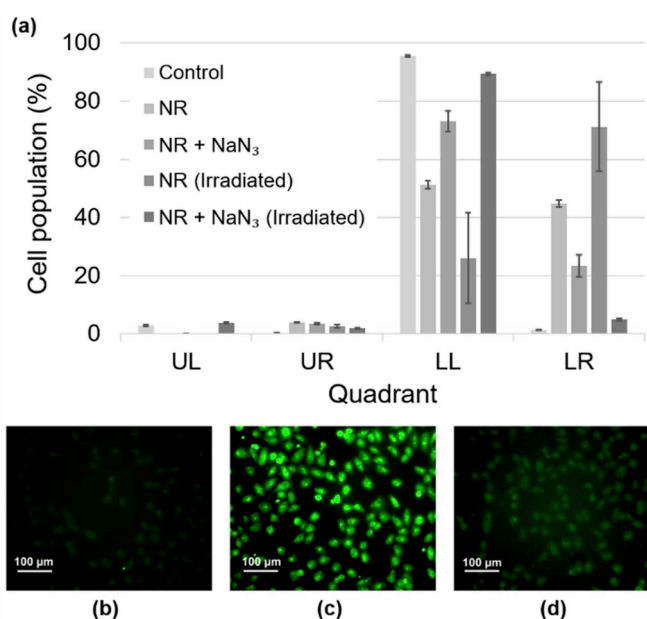


Fig. 3. Probe of mechanism of cell death through ROS level determination. (a) DCFH-DA assay for measurement of ROS levels in HeLa cells treated with Ag NRs in dark and under irradiation with and without sodium azide pretreatment. UL and LL represent ROS negative populations, whereas LR indicates maximum ROS positive population that is followed by UR. Data is represented as mean and standard deviation from three independent experiments; Fluorescence microscopic images showing DCF fluorescence in (b) control HeLa cells, (c) HeLa cells treated with Ag NRs under irradiation with 632 nm light (without pretreatment of sodium azide) and (d) HeLa cells treated with Ag NRs under irradiation with 632 nm light (pretreated with sodium azide). Scale bar: 100 µm.

4. Conclusions

In summary, conjugation of PDT and diagnostic assay techniques were achieved in a portable format involving minimal components to deliver a capable theranostic device. Interestingly, low irradiations doses from LEDs (1.4 mW/cm² at 632 nm) were found to be sufficient to impart efficient PDT and combinatorial therapy in HeLa cells and spheroids using Ag NRs as photosensitizers with an IC₅₀ dose of 2.5 µg/mL of Ag. The MTT and LDH measurements for treatment assessment indicated capability of device to perform reliable colorimetric assays. Smartphone based POC platforms have been applied for colorimetric detection, but the current work presented an advanced platform to perform therapy and diagnosis on a single device. As a future scope, the device can be also exploited for high-throughput screening of new photosensitizers and to perform other biochemical assays in disease diagnostics.

Declaration of competing interest

The authors declare the following financial interests/personal relationships which may be considered as potential competing interests: This manuscript has not been submitted elsewhere for consideration and all the authors have consented to the publication of the manuscript in your journal. An Indian patent application has been filed based on this work. (Application No. 201731031603 A).

CRediT authorship contribution statement

Sunil Kumar Sailapu: Conceptualization, Methodology, Software, Validation, Formal analysis, Investigation, Writing - original draft, Visualization. **Deepanjalee Dutta:** Conceptualization, Methodology, Validation, Formal analysis, Investigation, Writing - original draft,

Visualization. **Anitha T. Simon**: Investigation, Visualization, Writing - original draft. **Siddhartha Sankar Ghosh**: Conceptualization, Methodology, Validation, Supervision, Project administration, Funding acquisition. **Arun Chattopadhyay**: Conceptualization, Methodology, Validation, Writing - original draft, Supervision, Project administration, Funding acquisition.

Acknowledgement

We thank the Department of Electronics and Information Technology (No. 5(9)/2012-NANO (Vol. II)) and Centre for Excellence, DBT (Department of Biotechnology) programme support, Government of India for financial support.

Appendix A. Supplementary data

Supplementary data to this article can be found online at <https://doi.org/10.1016/j.bios.2019.111745>.

References

- Berg, B., Cortazar, B., Tseng, D., Ozkan, H., Feng, S., Wei, Q., Chan, R.Y., Burbano, J., Farooqui, Q., Lewinski, M., Di Carlo, D., Garner, O.B., Ozcan, A., 2015. *ACS Nano* 9, 7857–7866.
- Dhawan, A.P., 2016. *IEEE J. Transl. Eng. Health Med.* 4, 2800908.
- Dutta, D., Sahoo, A.K., Chattopadhyay, A., Ghosh, S.S., 2016. *J. Mater. Chem. B* 4, 793–800.
- Guo, H.W., Lin, L.T., Chen, P.H., Ho, M.H., Huang, W.T., Lee, Y.J., Chiou, S.H., Hsieh, Y. S., Dong, C.Y., Wang, H.W., 2015. *Photodiagn. Photodyn. Ther.* 12, 504–510.
- Hartl, B.A., Hirschberg, H., Marcu, L., Cherry, S.R., 2015. *Biomed. Opt. Express* 6, 770–779.
- Huang, P., Xu, C., Lin, J., Wang, C., Wang, X., Zhang, C., Zhou, X., Guo, S., Cui, D., 2011. *Theranostics* 1, 240–250.
- Huang, X., Tian, X.J., Yang, W.L., Ehrenberg, B., Chen, J.Y., 2013. *Phys. Chem. Chem. Phys.* 15, 15727–15733.
- Jadhav, K., Deore, S., Dhamecha, D., H R, R., Jagwani, S., Jalalpure, S., Bohara, R., 2018. *ACS Biomater. Sci. Eng.* 4, 892–899.
- Komarova, N.L., Boland, C.R., 2013. *Nature* 499, 291–292.
- Kwon, L., Long, K.D., Wan, Y., Yu, H., Cunningham, B.T., 2016. *Biotechnol. Adv.* 34, 291–304.
- Luka, G.S., Nowak, E., Kawchuk, J., Hoorfar, M., Najjaran, H., 2017. *R. Soc. Open Sci.* 4, 171025.
- Merlin, J.L., Azzi, S., Lignon, D., Ramacci, C., Zeghari, N., Guillemin, F., 1992. *Eur. J. Cancer* 28, 1452–1458.
- Muller, P.J., Wilson, B.C., 1986. *Phys. Med. Biol.* 31, 1295–1297.
- Nahabedian, M.Y., Cohen, R.A., Contino, M.F., Terem, T.M., Wright, W.H., Berns, M.W., Wile, A.G., 1988. *J. Natl. Cancer Inst.* 80, 739–743.
- Popp, M.K., Oubou, I., Shepherd, C., Nager, Z., Anderson, C., Pagliaro, L., 2014. *J. Nanomater.* 1–8, 2014.
- Rodrigues, J.A., Amorim, R., Silva, M.F., Baltazar, F., Wolffenbuttel, R.F., Correia, J.H., 2019. *IEEE J. Sel. Top. Quantum Electron.* 25, 1–6.
- Vankayala, R., Huang, Y.K., Kalluru, P., Chiang, C.S., Hwang, K.C., 2014. *Small* 10, 1612–1622.
- Yogo, T., Urano, Y., Ishitsuka, Y., Maniwa, F., Nagano, T., 2005. *J. Am. Chem. Soc.* 127, 12162–12163.
- Zhang, M., Liu, E., Cui, Y., Huang, Y., 2017. *Canc. Biol. Med.* 14, 212–227.